Simulation of Soot Filtration on the Nano-, Micro- and Meso-scale

L. Cheng[1], S. Rief[1], A. Wiegmann[1], J. Adler[2], L. Mammitzsch[2] and U. Petasch[2]

[1]Fraunhofer-Institut Techno- und Wirtschaftsmathematik, Fraunhofer-Platz 1, 67663 Kaiserslautern, Germany

[2]Fraunhofer-Institut für Keramische Technologien und Systeme, Winterbergstr. 28, 01277 Dresden, Germany

Abstract

The pressure drop evolution incurred in diesel particulate filters during the soot loading cycle is an important quantity of interest for the automotive industry. It is influenced by the shape of the filter, the pore geometry in the filter walls and even the precise soot deposition patterns inside these pores. We simulate and try to understand these processes by considering three different scales. On the scale of soot particles, simulations help determining packing densities of soot cake in the pores and on top of the ceramic filter media. On the scale of the filter media, simulations help determine depth and cake filtration parameters as function of deposited dust or time. Figure 1 illustrates the connection of rather free flow in the earliest stages of the filtration, the onset of clogged channels throughout the material and finally, cake filtration, with the typical S-curves observed in many measurements. In this case, comparison with experiments yields the viscous flow resistivity of the channel cake and surface cake.

With these parameters, also the depth and cake filtration on the scale of honeycomb structures can be simulated and understood.

Keywords: Soot filtration, multi-scale, simulation, modelling, CFD

1. Introduction

The goal of this work is ultimately to use computer simulations to find a diesel particulate filter with better filtration properties, i.e. lower pressure drop, higher efficiency, and longer life time. Along the way towards this goal, the ceramic filter media was identified as one of the key ingredients that govern the DPF performance. So, as a step along the way, in this work we demonstrate that an improved ceramic filer media can be predicted by simulations. Many ingredients of the simulation such as the ceramic media models, the computation of the air flow, tracking the particles, and depositing the particles and converting them to a porous media were established in our previous work. Here, a multivariate resistivity model is introduced and shown to allow the prediction of pressure drop measurements after first fitting the two key parameters in the model, namely maximal soot packing density and corresponding maximal flow resistivity against pressure drop measurements. As intermediate step,

three different ways of estimating these key parameters are described and found to disagree significantly, raising some new questions to be investigated in the future. One way to find the two parameters are nano-scale simulations. How to use these parameters also on the honeycomb scale is hinted at in the meso-scale consideration part of this article.

2. Air flow simulation

The Navier-Stokes-Brinkman equations (see Figure 1.) are used in the filtration simulations on all three scales. In the filtration context, they were introduced by Iliev and Laptev[1]. On the nano-scale, when the soot particles are resolved by the computational grid, the Brinkman term involving the porous voxel permeability κ is not needed, and just the Navier-Stokes equations are used, usually simplified to the Stokes equations by also dropping the nonlinear (inertia) term. On the media scale the Brinkman term is active in cells where soot has deposited. On the honeycomb scale, the Brinkman term is active in cells representing the walls and gets modified where soot deposits in the walls or on top of the walls.

$$
\begin{aligned}
-\mu\Delta\vec{u} + \nabla\vec{u}\cdot\vec{u} + \kappa^{-1}\vec{u} + \nabla p &= \vec{\mathrm{f}} \text{ (momentum balance)} \\
\nabla\cdot\vec{u} &= 0 \text{ (mass conservation)} \\
\vec{u} &= 0 \text{ on } \Gamma \text{ (no-slip on fiber surfaces)}
\end{aligned}
$$

$\vec{\mathrm{f}} = (0,0,f)$: force in flow(z)-direction,
κ : porous voxel permeability,
$\vec{u}$: velocity,
μ : fluid viscosity,
p : pressure and
Γ : surfaces of fibers or deposited particles.

Figure 1. Navier-Stokes-Brinkmann equations and notation.

3. Soot transport simulation

Figure 2 gives the precise formulation for the particle transport without collisions in the most general form. As the soot particles are tracked with the air, two terms contribute to the particle velocity. The radius and density (as mass) enter into the friction of the particle against the flow, and also into the diffusive part of the motion.

$$
\begin{aligned}
\frac{d\vec{v}}{dt} &= -\gamma\times(\vec{v}(\vec{x}) - \vec{v}_\circ(\vec{x})) + \frac{Q\vec{E}_\circ(\vec{x})}{m} + \sigma\times\frac{d\vec{W}(t)}{dt} \\
\frac{d\vec{x}}{dt} &= \vec{v} \\
\gamma &= 6\pi\rho\mu\frac{R}{m} \\
\sigma^2 &= \frac{2k_BT\gamma}{m} \\
\left\langle dW_i(t), dW_j(t)\right\rangle &= \delta_{ij}dt
\end{aligned}
$$

t: time
$\vec{x}$: particle position
$\vec{v}$: particle velocity
R: particle radius
m: particle mass
Q: particle charge
T: ambient temperature
k_B: Boltzmann constant
$d\vec{W}(t)$: 3d probability (Wiener) measure
$\vec{E}_\circ$: electric field
$\vec{v}_\circ$: fluid velocity
ρ: fluid density
μ: fluid viscosity

Figure 2. Lagrangian description of particle motion.

Electrostatic charges are in principle possible in the simulations, but not active here. Particles can be positioned anywhere in space, while the fluid velocity is only available at a discrete set of points in space, for example on cell walls in case of one particular finite difference solver. To approximate fluid velocities at all particle locations, these discrete velocity values are linearly interpolated.

4. Soot particle deposition and conversion to porous media

The flow and collision models account for most mechanisms of filtration: except for the influence of their mass and electric charges, particles follow the streamlines and can be caught by **direct interception**. Due to their mass, they can leave stream lines and can be caught by **inertial impact**. For small particles, as is the case for soot, the effect of Brownian motion is significant, and they can be caught by **diffusive deposition**.

Because the particles are spherical, only the distance of the particle center from the nearest obstacle needs to be computed in order to detect collisions. To further accelerate this computation, the media model is equipped with a so-called distance function, which provides information about the distance to the nearest obstacle voxel for all empty voxels. If the particle radius is smaller than the distance function value at its position, then no collision can occur. In case of soot, the other situation is rather simple – the soot is assumed to be completely sticky, i.e. soot deposits on first contact. Two cases must be distinguished. When the computational grid for the flow simulations resolves the particles, particle deposition simply turns previously empty grid cells into solid grid cells. More interestingly, when the grid does not resolve the particles, a depositing particle adds mass to the cell and the cell becomes porous. The key contribution of this article is determining the maximal achievable density and corresponding maximal flow resistivity in this unresolved setting.

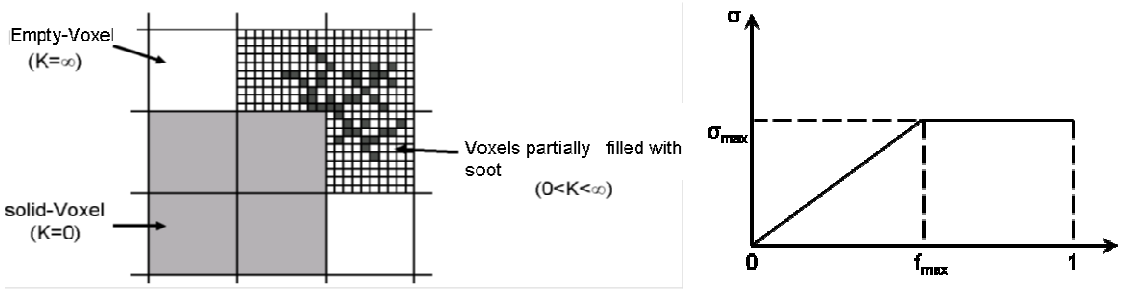

Figure 3. Soot deposited voxels are considered porous (left). The resistivity of the voxels is depends linearly on the solid volume fraction (right).

In general, for porous media with low porosity, it is a standard assumption that flow resistivity depends linearly on the solid volume fraction. In our model, this linear relation is assumed up to a maximum packing density f_{max}, beyond which no more soot particles can enter a computational grid cell. Thus, the two independent parameters of the model are the maximal packing density of a cell and the flow resistivity of the cell at this packing density. In the graph on the right of Figure 3, these mean the end point of the diagonal line and the slope of this line. Since numerically also packing densities slightly larger than f_{max} may occur, we continue the relation as constant for $f > f_{max}$.

$$\kappa = \frac{\mu}{\sigma}, \qquad \sigma = \begin{cases} \frac{f}{f_{max}} \sigma_{\max}, & 0 < f < f_{\max} \\ \sigma_{\max}, & f \geq f_{\max} \end{cases}$$

Since the Navier-Stokes Brinkman equations are written in terms of the permeability κ, the relation of permeability and resistivity is also spelled out. In the new multivariate permeability model, σ_{max} is different for depth filtration, denoted by σ^1_{max} and cake filtration, denoted by σ^2_{max}.

5. Determining packing density and flow resistivities

The first way to determine f_{max} and σ_{max} is by resolved scale simulations. In [2], Rief et al performed such calculations on grid with 20 nm resolution, so that soot particles of 80nm were resolved by the grid. Figure 4 shows such soot particles deposited on a single 4µm fiber (with diameter 200 grid cells), and on the right a cut-out of the layer of soot particles. By analyzing this layer, a maximum packing density f_{max} = 0.15 and a permeability of 10^{-3} Darcy or κ = 1e-15 m^2 were found. Using, as we do throughout this article, the fluid viscosity µ = 1.834e-5 kg/m/s, yields σ_{max} = 1.834e10 kg/m³/s.

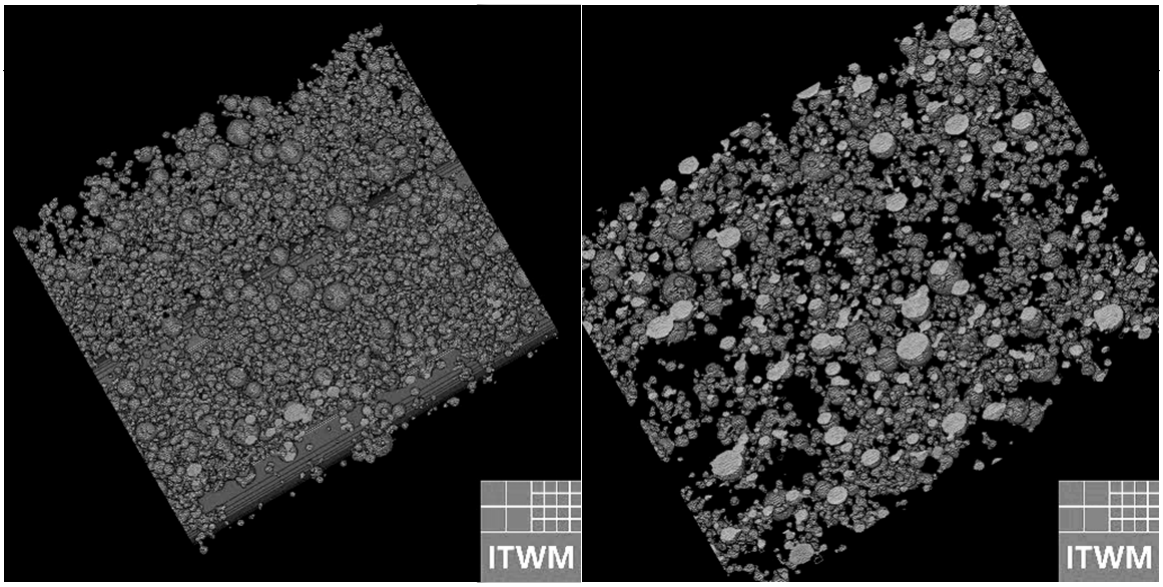

Figure 4. Soot deposited on a fiber in 20nm scale simulations (left). Cut through the resulting soot cake, from which f_{max} = 0.15 and κ = 1e-15 m^2 were found (right).

A second way to determine f_{max} and σ_{max} is by measuring cake height and pressure drop as functions of deposited soot. At Fraunhofer IKTS, soot was deposited on flat ceramic samples at different flow rates. Figure 5 shows the test rig where the samples were loaded with soot. The loading was stopped after different times, and the height of the soot cake on top of the ceramic was measured. Figure 6 depicts the thickness of a layer of soot depositing on a flat ceramic sample with the diameter 46 mm. The computed bulk density from the fitted linear trend line is 175 kg/m^3. The soot density is 1700 to 1900 kg/m^3. From this, one estimates f_{max} = 0.1. This is about 33% lower than the value used in [1]. Since the test rig in Figure 5 also measures the pressure drop as a function of deposited dust, it is also possible to estimate the flow resistivity, here σ_{max} = 2.64091e08 kg/m³/s.

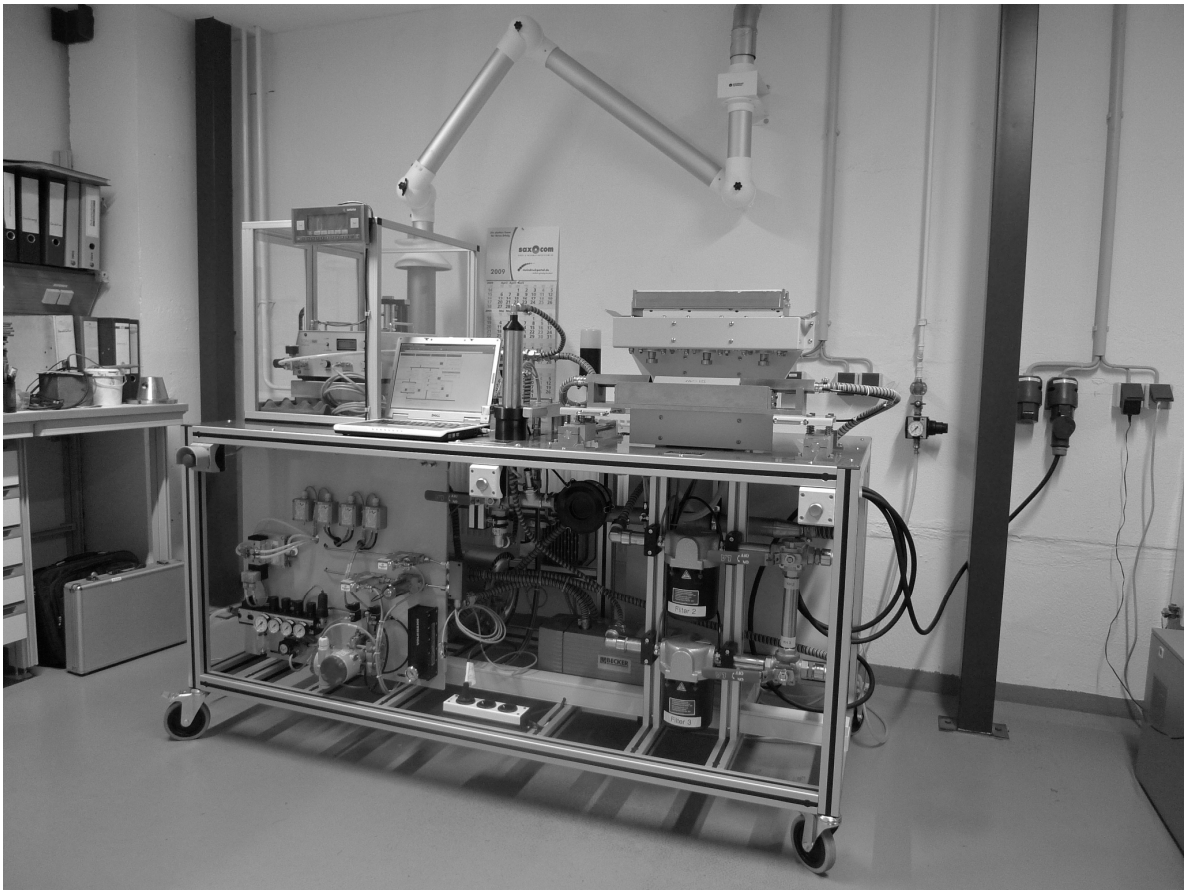

Figure 5. Test rig for soot deposition on flat ceramic samples.

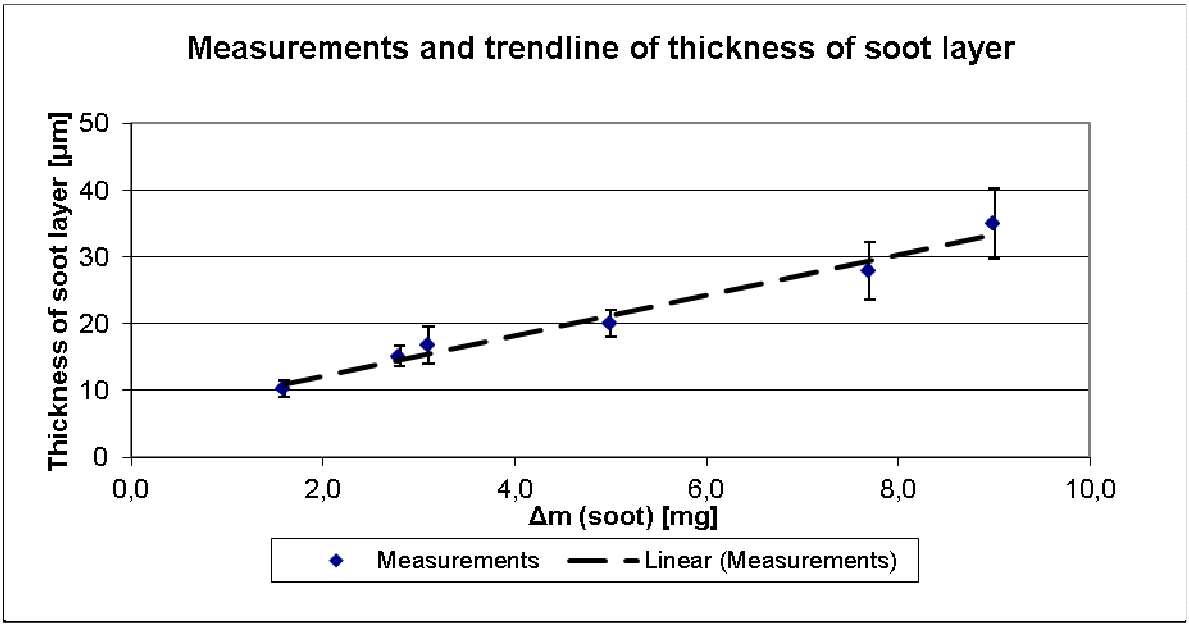

Figure 6. Thickness of a layer of soot depositing on a flat ceramic sample with diameter 46 mm.

The third and last way to determine f_{max} and σ_{max} is to fit the simulation parameters in a media scale simulation until the predicted pressure drop agrees with the experimental data. In order to proceed, first a detailed ceramic model must be made.

Following our earlier work [3, 4], and building on SEM images, such models were created for two different ceramics: NTF_S and NTF_B. Figure 7 shows SEM and virtual SEM (vSEM) of NTF_S, and also illustrates that there actually exists a 3d ceramic model, with the possibility to deposit soot in depth and on top of this ceramic.

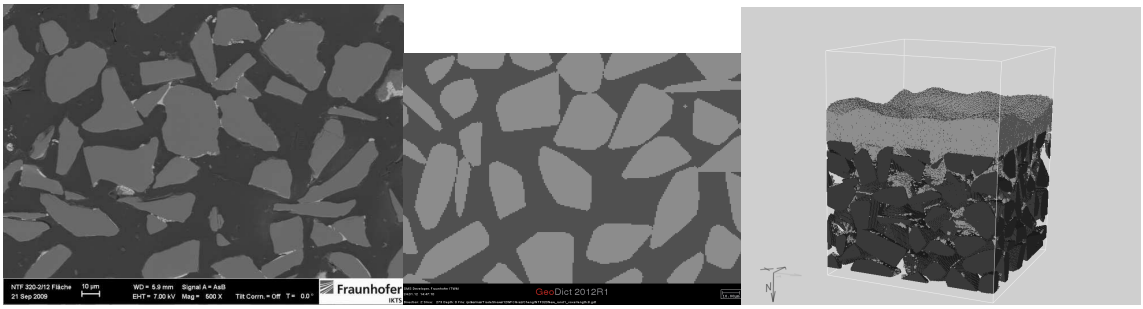

Figure 7. SEM, matching vSEM, and 3d view of virtual ceramic media, the latter also depicting deposited soot after depth and cake filtration in light gray.

One way beyond comparing SEM and vSEM to ensure that the 3d structure of the model really agrees with reality is to compare the pore size distribution. Figure 8 shows the good agreement, albeit the peak in the pore size distribution in the model is significantly higher than that in mercury porosimetry measurements of the real ceramic.

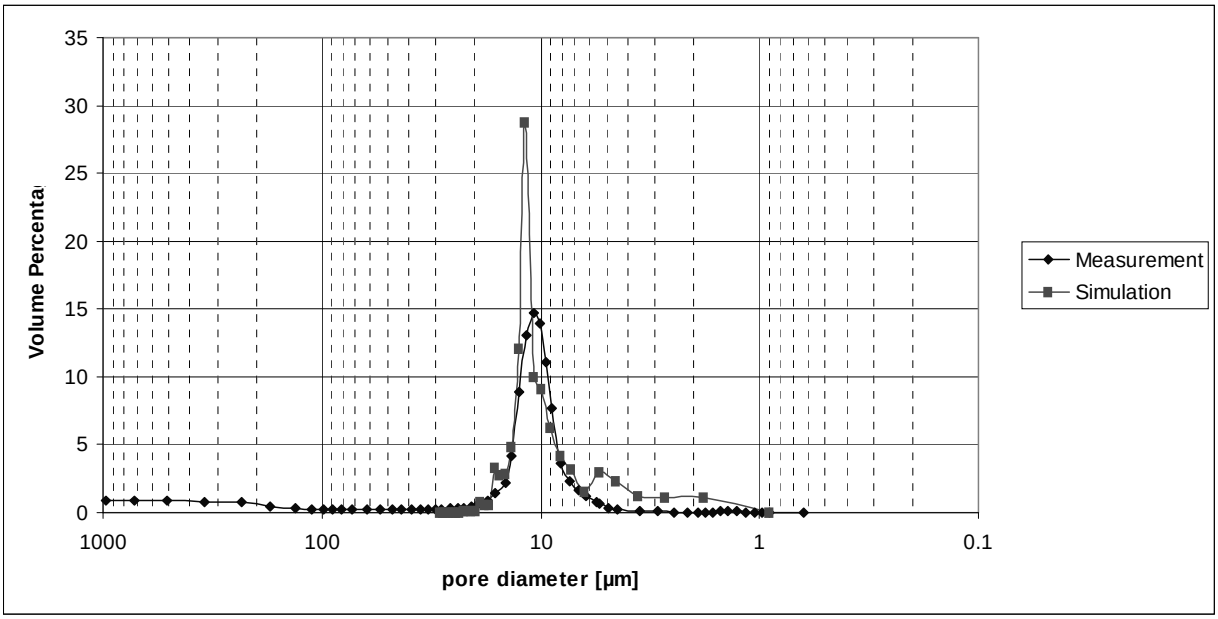

Figure 8. Experimental and simulated pore size distribution of media in Fig. 7.

Figure 9 shows the experimental data to which f_{max} and σ_{max} can be fit. Two phases, depth and cake filtration can be clearly distinguished, and make it seem reasonable that different sets of parameters may be needed for the two phases. 3 parameters can be extracted: the slopes of the pressure drop over time in depth and cake filtration, *s1* and *s2*, and the moment in time / amount of soot *x* for which the behavior changes from depth to cake filtration. As a closing assumption, we assume f_{max} to be the same for both phases, and are left with the need to fit $f_{max,}$ σ^1_{max} and $\sigma^2_{max.}$ This assumption is partially based on the fact that the experimental pressure drop curves,

when scaled by the fluid velocity, all agreed to be on a master curve – at least for the relatively low mass flow rates under consideration. We concluded that the soot packing density has to be independent of the flow velocity, and should thus be the same in the pores of the ceramic as in the soot filter cake on top of the ceramic.

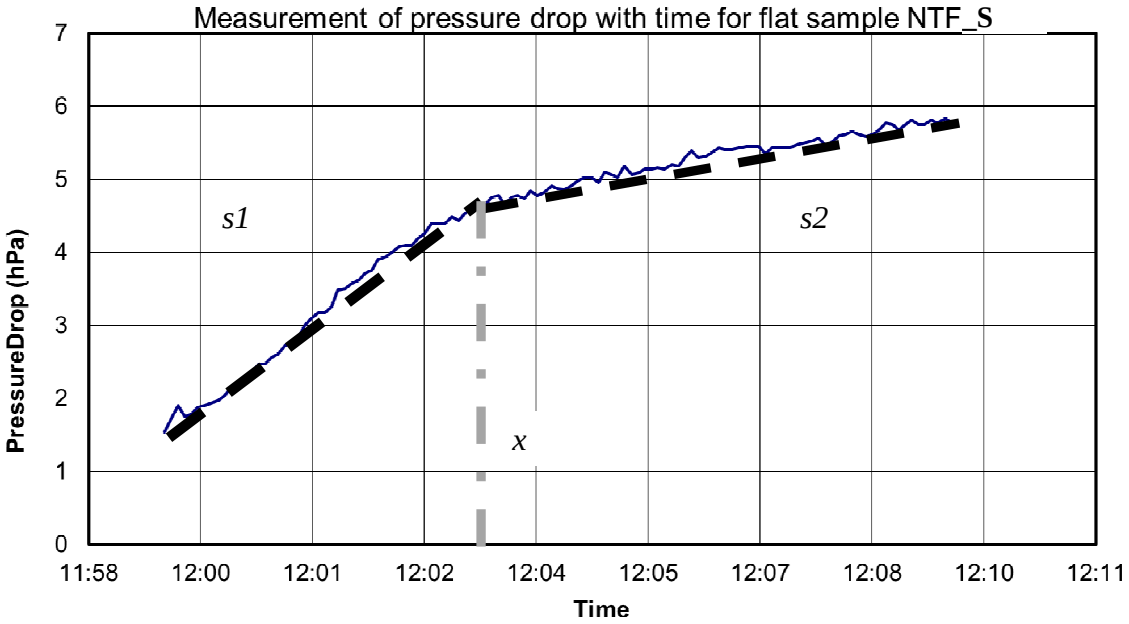

Figure 9. Evolution of the pressure drop over time, as soot is depositing on the flat NTF_S sample. By assuming a uniform concentration of soot, these experimental data can also be converted into pressure drop as a function of deposited soot. Two phases can be clearly distinguished. Phase 1, with slope *s1*, where depth filtration occurs and the soot enters into the ceramic, and phase 2 with slope *s2*, where the soot deposits as cake on top of the ceramic. The transition point *x* is the moment in time or amount of deposited soot, respectively, where the change from depth to cake filtration occurs.

In the simulations, we varied these three quantities until the simulated pressure drop curve fit with the experimental ones. As the soot consisted of agglomerated particles, the density used in the simulation was 150 kg/m^3, σ_{max} for the depth and cake filtration are σ^1_{max} = 3.5e+8 kg/m³/s and σ^2_{max} = 8.8e+7 kg/m³/s, respectively, and f_{max} is 0.45. These data deviate significantly from those in [1], where σ_{max} was estimated to be 1.834e10 kg/m³/s. The difference in f_{max} is not as large as it seems at first, because [1] considered primary particles, whereas on this scale we use agglomerates. Expressed with respect to the density of in primary particles, 0.45 * 150/1800 = 0.0375, our simulation value is even lower than the one estimated from the cake height. Figure 10 shows the pressure drop evolution both for 5 experiments and for 5 simulations runs, i.e. 5 different realizations of the ceramic model. The error bars on the simulation data are narrower than for the experimental data. This indicates that the small cutouts of the ceramic considered in the simulation are more homogeneous than the true ceramic – a typical phenomenon observed in several of our material simulation projects.

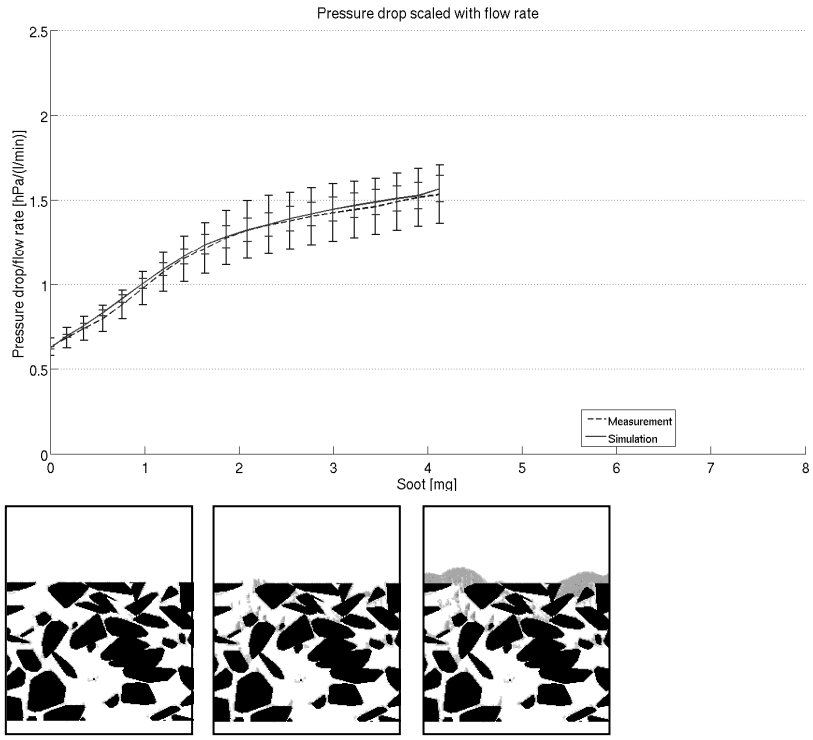

Figure 10. Experimental and simulated pressure drop evolution with error bars induced by 5 measurements and 5 different realizations of the virtual structure. The cross sections indicate the empty structure used to compute the initial pressure drop, the depth filtration phase and the cake filtration phase. The variation for different simulation runs lies within the variation of the experimental data.

6. Predicting the pressure drop for a new DPF media

The parameters that were used to fit the NTF_S sample where then used to predict the behavior of NTF_B, a similar ceramic made from larger grains that result also in larger pores. Figure 11 shows the results of this prediction. Again, multiple experimental pressure drop curves are plotted, in this case not as mean curve with error bars but as individual curves. They were obtained by scaling the true measurements by the mass flow rate, and since no trend was observed in the data, we concluded that the simulation parameters could be used independent of the flow rates, at least in the slow flow regimes of the current experiments.

Two main conclusions can be drawn.

1. The maximum packing density and flow resistivities obtained for NTF_S also predicted very well the behavior of NTF_B and

2. The pressure drop of NTF_B is about 10% lower both in the simulation and in the experiment.

This means an important step in virtual material design is established – the behavior of not yet existing materials can be predicted by computer simulations, as long as the parameters were established and validated against measurements of media that are not too different from the new and virtual ones.

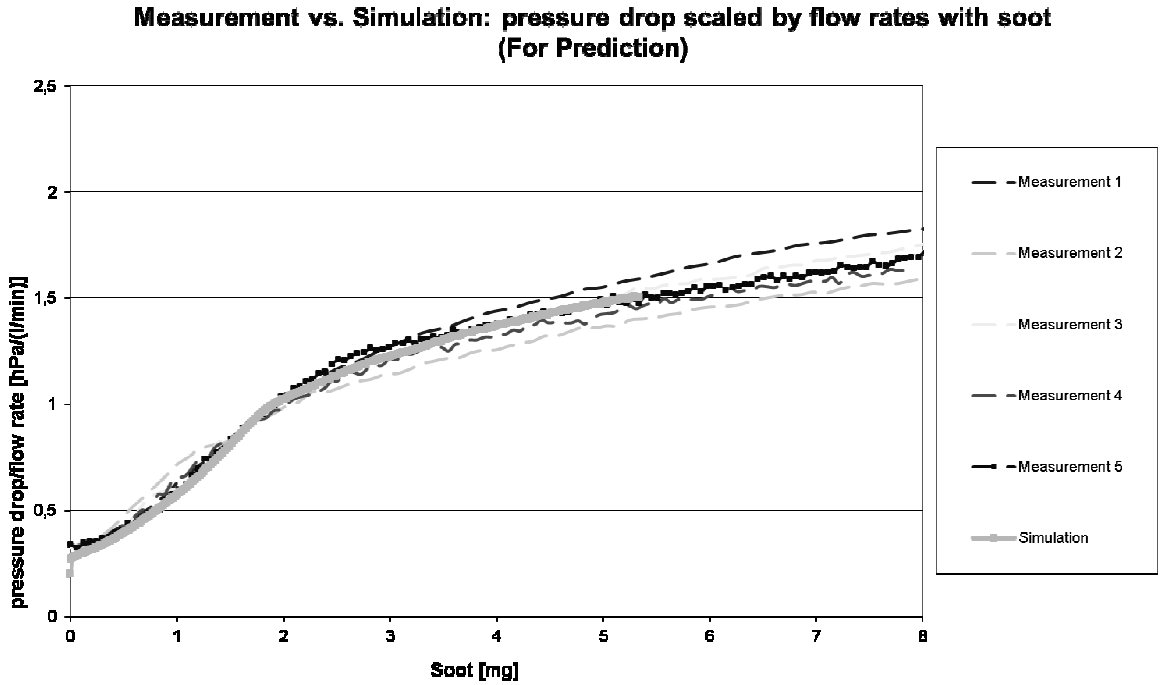

Figure 11. Experimental and simulated pressure drop for a different ceramic, with parameters found by fitting against the measurements in Figure 6. Due to the larger pores, depth filtration starts later, and the overall pressure drop is lower than for the media in Figure 6.

7. Outlook towards the macro scale

At the end of the day, what really matters in practice is the behavior of the complete filter and not just the filter media. The next scale under consideration along that way is that of honeycomb structures. Here, many designs such as channel shape, channel length, channel dimensions, wall thickness, plug behavior, etc. etc. matter. The same equations as on the nano and micro scales describe the air flow and the particle motion. Now, the ceramic must be modeled as porous media with density and permeability, and these may change as particles are deposited. A complex interplay of soot cake growth and channel diameter reduction add to the pressure drop in a way not considered for flat samples, and the sheer number of soot particles to be handled by the simulation grows from hundreds of millions on the media scale to hundreds of billions on the honeycomb scale. Figure 12 shows the approach and some stream lines, but the fundamentally different deposition mechanism of particles not being collected on a surface but randomly inside the filter media still awaits a solution, at least in the currently described simulation framework GeoDict.

8. Conclusions

We found that using two different values for the maximal flow resistivity, in the depth filtration phase and the cake filtration phase, the simulations could be matched precisely to measurements on one DPF media, and then these parameters predicted extremely well the pressure drop of another, not to different but better DPF media. This work confirms an important step in virtual material design – the behavior of not yet existing materials can be predicted by computer simulations, as long as the parameters were established and validated against measurements of media that are not too different from the new and virtual ones.

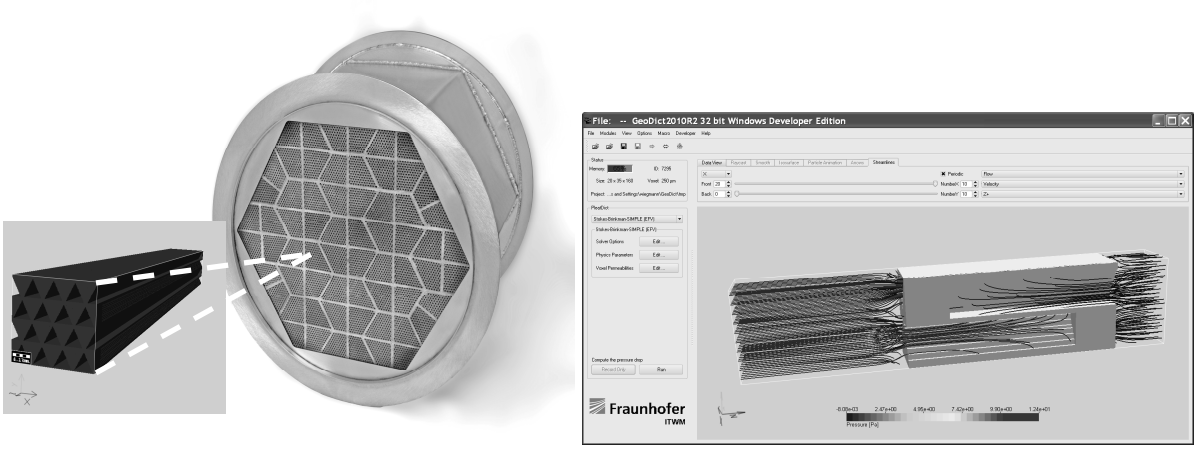

Figure 12. Honeycomb structure with simulated detail and lines / particle trajectories.

9. Acknowledgements

We thank the Fraunhofer Society for funding in the FeiFilTools MEF project and Kilian Schmidt for his contributions in the early stages of that project. All media, flow, filtration and honeycomb simulations were carried out with the GeoDict Software [5].

References

[1] O. Iliev, V. Laptev. *On Numerical Simulation of Flow through Oil Filters*, J. Computers and Visualization in Science, vol. 6, 2004.pp. 139-146.

[2] S. Rief, D. Kehrwald, A. Latz, K. Schmidt, A. Wiegmann. *Virtual Diesel Particulate Filters: Simulation of the Structure, Exhaust Gas Flow and Particle Deposition*. Filtration, No. 4, Vol. 9, 2009, pp. 315-320.

[3] A. Wiegmann, S. Rief, A. Latz. *Soot Filtration Simulation - Generation of Porous Media on the Micro Scale from Soot Deposition on the Nano Scale*, Proceedings of the 2nd European Conference on Filtration and Separation, Compiegne, France, October 2006, pp. 141-147.

[4] S. Rief, D. Kehrwald, K. Schmidt, A. Wiegmann. *Simulation of ceramic DPF media, soot deposition filtration efficiency and pressure drop evolution*, Proceedings of the 10th World Filtration Congress, III-318, Leipzig, April 2008.

[5] J. Becker, E. Glatt, A. Wiegmann, GeoDict, http://www.geodict.com, 2012.